Proceedings of the Korean Nuclear Society Spring Meeting
Kwangju, Korea, May 2002

Preliminary Analysis of CABRI LTX Test using SAS4A Code

Soo-Dong Suk
Korea Atomic Energy Research Institute
150 Dukjin-dong, Yusong-gu, Daejeon, Korea 305-353

Ikken Sato
Japan Nuclear Cycle Development Institute
4002 Narita, Oarai-machi, Higashi-Ibaraki-gun, Ibaraki, 311-1393 Japan

Abstract

The LTX test was performed using a SCARABIX pin in March 2000 in the framework of the CABRI RAFT Program to investigate the pin failure mechanism, in-pin fuel motion and post-failure fuel relocation behavior under a simulated TUCOP accident in LMFR. The transient of the test was initiated by a coolant flow reduction and a structured TOP was triggered when coolant average temperature at TFC reached a predefined value to keep the channel in the subcooled condition. Pin failure occurred rather early, before the initiation of any significant fuel melting. Rapid gas release upon the cladding failure led to the voiding of coolant channel, followed by a molten fuel ejection and gradual axial relocation in the test channel.

An effort was made to interpret the experimental results of the LTX test using the SAS4A code. Although the original SAS4A model was not well fitted for this type of early pin failure, the global behavior after the pin failure was reasonably simulated with time and axial location of the pin failure specified as an input to the code and judicious choice of failure criteria.

1. Introduction

The LTX test was performed in March 2000 as part of the CABRI RAFT Program. The objectives of the test were to investigate the pin failure mechanism, in-pin fuel motion and post-failure fuel relocation behavior under a TUCOP(Transient Undercooling Overpower) in sodium coolant channel. The test conditions are essentially the same as those of the preceding LT4 test[1], which had been carried out in March 1997 in the framework of the CABRI FAST program.

The transient of the test was initiated by a coolant flow reduction from the steady-state value of 135 g/s with a halving time of about 7 seconds. A programmed transient overpower(TOP) was then triggered at 18.5 sec after the initiation of loss of flow(LOF) when coolant average temperature at the fissile top reached a predefined value to keep the channel in the subcooled condition. Extensive azimuthal temperature oscillations were observed during the LOF and a local onset of sodium boiling took place during the pre-pulse period of the TOP.

A cladding failure occurred rather early at around 460 ms after TOP, before any

significant fuel melting initiated. Upon the cladding failure, a rapid gas release led to an extensive coolant-channel voiding. Under the circumstances, the continued power transient in the test gave rise to progressive fuel melting and subsequent axial relocation of molten fuel similar to the other CABRI TUCOP tests with extended coolant boiling conditions. Because of limited energy injection, fuel disruption and axial relocation were finally contained within the fissile region. A significant blockage of the test channel appeared after the transient, with a flow rate reduced to 3 % of the initial flow.

In this study, the SAS4A code, version "REF99 Release 3, is utilized to simulate the sequence of events through the transients of LOF and TOP as well as the pre-irradiation history and steady state power operation. The focus is made, however, on demonstrating the limitations as well as the ability of the code to predict the post-failure fuel behavior in the TUCOP test like the LTX.

2. Major Test Features and Results

A structured TOP was automatically triggered when the mean sodium temperature at TFC reached 893℃ with sodium flow rate decreased to 40 g/s. Figure 1 shows the power history during the TOP. At the end of pre-pulse(480 ms after the TOP onset), energy release at the peak power node (PPN) was increased to 0.49 kJ/g. Its value reached up to 1.11 kJ/g at the time of scram(720 ms), and saturated to 1.23 kJ/g by the end of the TOP(1.2 s). Transient power increased by 45.4 times the steady-state power at 543 ms after the onset of TOP.

A SCARABIX pin was used in the LTX test as in the LT4 test. The pin is a mixed-oxide annular fuel pellets of 21.4% Pu /U+Pu pre-irradiated in PHENIX to a local burnup of 6.4 at.%, clad in 15/15 Ti with an outer radius of 8.5 mm and axial fissile length of 75 cm. For the LTX test, modifications were made on the test pin used in the LT4 test by replacing original solid fertile pellets by hollow insulation pellets. This is to study in-pin fuel motion expected to take place during the test, particularly the fuel squirting before cladding failure toward the gas plena through the central holes connecting the fissile region and gas plena. A new device, DT (Displacement Transducer), was installed just above TFC(Top of Fuel Column) to detect the squirted fuel moving upward from the fissile.

During LOF of the test, the elongation of fissile fuel of 2 ($\pm$2) mm was observed by the neutron hodoscope, while it was 3($\pm$2) mm in the LT4 test. Although relatively large uncertainty in the measurements makes a direct comparison of the fuel elongation difficult, the slight difference is consistent with more extensive pin bending expected in the LTX test than in the LT4 test. An analysis[2] of the LTX test using the PAPAS-2S code shows that the earlier cladding failure could be due mainly to local cladding heat-up and stress concentration caused by excessive pin bending occurred in the LTX test. The peak coolant temperature took place at about 60cm from BFC(Bottom of Fuel Column) during the TOP, while it was around TFC in the LT4 test.

Figure 2 shows test data of sodium flow rates during TOP, compared to the results obtained using SAS4A code. Local sodium boiling began at around 410 ms after TOP during the pre-pulse in 60cm from BFC(Bottom of Fuel Column), leading to a moderate sodium expulsion from the channel. A more violent sodium expulsion transient took place at 460 ms, before onset of the main pulse, apparently caused by the cladding

failure and subsequent gas release. Unfortunately, some important instrumentation malfunctions took place during the test. Due to some unsuitable configuration as well as connectivity problems, the microphone and the pressure measurements failed. As a result, precision was lost for the timing of the rupture events and their locations.

Various events of measurement are shown along with the flowmeter integral curve in Figure 3. After the peak of the main pulse (560 –670 ms), the progressive destruction of the TCs(thermocouples) in the test channel near the presumed rupture location (on the levels of 30, 45, 60 cm BFC) indicated the fuel ejectionl. In the mean time, the DT caught a dynamic event at 526 ms. About 4 ms later, the hodoscope registered a signal increase at TFC. However, the PTE(Post-test Examination) did not reveal any sign of in-pin molten fuel relocation above TFC. The DT event and subsequent hodoscope event are considered, therefore, to have been upward motion of the upper part of the pin. The squirting detection device was also found in the original unreleased state. There were no correlated TC events at TFC.

Final state of the test fuel deduced from the hodoscope data shows the trend of the fuel accumulation around TFC and in the upper zone, noticeable lack of fuels in the mid-zone, and accumulation in the bottom part of the fuel. Results of the post-test non-destructive examinations by gammametry and X-ray images are in general agreement with the trend described in the above. It was also shown that the clad had been severely damaged and not visible between 31.3 and 59.6 cm, the pin nose had been displaced in the upward direction by 17 mm. No molten fuel was observed in the central hole above or around TFC.

3. Analysis Assumptions and Bases

3.1 Failure Specifications and Criteria

There are three major events of fuel pin failure in simulating the molten fuel behavior using the SAS4A code. They include cladding failure and gas release, pin failure(fuel melting causing cladding rip-off or separation), and fuel disruption, which take place simultaneously or in sequence depending on the specific transient. Since the major interest of this study is the molten fuel behavior after clad failure, the time and axial locations of the clad failure were specified as inputs to the code in this study, based on the interpretation of the test data.

First, it is assumed for the analysis that clad failure occurred at around 60 cm above BFC at 460 ms after the onset of TOP. There seems to be no direct measurement to indicate where it failed in the test. However, test data, shown in Figure 2 indicates time of the clad failure as evidenced by a rapid flow-rate divergence. As described in Section 2, the peak sodium temperature occurred at 60cm BFC rather than at TFC seemingly because of an excessive pin bending occurred in the test. It is deduced from the experimental data and analysis with PAPAS-2S that the cladding mid-wall temperature at the hottest TC azimuth of 60cm BFC reaches beyond 1050℃ by the time of 460 ms after the TOP onset. At this temperature level, the cladding hoop stress corresponding to the plenum gas pressure could be enough to induce cladding failure.

Secondly, it is basically assumed in the analysis that the molten fuel ejection occurs at 526 ms upon the onset of TOP at 60cm BFC, the axial location of cladding failure. Based on the DT signal at 526 ms/ TOP and subsequent hodoscope event, and the PTE

results as well, the following sequence of events are assumed to have occurred around the time of pin failure ; Fuel pin separation takes place at 526 ms by losing the strength at the axial location of around 60 cm BFC, where the upper edge of melt front of the fuel is reaching at the time of failure. The upper pin separated from the lower one moves upward into the free space above the pin and stays there during the test.

Finally, fuel disruption is expected under a rapid cladding heat-up and fuel melting after the fuel ejection. Criteria for fuel disruption are 20 % AMF(fuel areal melt fraction) and cladding midwall temperature of 1250 °C, as used in the previous studies with SAS4A. It should be noted that this cladding-temperature level is usually reached just after cladding dryout in the conventional situations.

3.2 Plenum-Gas Blowout Model

In the SAS4A model, failure prediction is linked to the ejection of molten fuel and its interaction with sodium and coolant-channel structures. For the condition of single-phase coolant , therefore, cladding failure is allowed only after some amount of fuel melting gets available. Under the circumstances, the plenum-gas blowout model, usually applied after coolant boiling, had been used for simulating early cladding failure and subsequent gas release in the studies with the SAS4A code. In order to simulate the LTX test, some modifications were necessary to correct the inconsistency handling the condensation of gas mixture between the pre- and post-failure models. Input parameters specifically selected in this study are essentially same as those used in the SAS4A analysis of the LT1 study [3] for the condition of single-phase coolant.

4. Analysis Results

4.1 Pre-Failure Analysis

A set of major input variables of SAS4A were prepared based on the test conditions, which include power history normalized to the steady-state power, axial power distribution during the steady state and flow rate during LOF, among others. The steady-state conditions such as coolant temperature distribution along the channel were well simulated with the code. Figure 4 shows a comparison of the coolant temperature history at TFC during LOF between the TC data and the analysis result by the code. It can be noticed that there exist variations of the TC signals presumably because of pin bending, which is not modeled in the SAS4A code. Pin bending appears to cause the trend of a slight underestimation of the coolant temperature by the code.

Figures 5 presents comparison of coolant temperature histories measured by TCs at various azimuthal angles with the analysis results at TFC during the early phase of the TOP. As can be seen in the figures that the coolant heat-up behavior is well simulated by the code during TOP up to the time of cladding failure. It may be noted that the calculated coolant temperature at TFC temporarily decreases from 940℃ at 526 ms upon the onset of TOP as much as 40℃ just prior to the step increase up to 1,270℃. On the other hand, the coolant temperatures measured by TCs slowly increases toward the saturation temperature. As described in the analysis report of the LT1 test[3], a sudden dip of the temperature arises from the upward motion of the relatively cold coolant slug from down below. The absence of coolant temperature drop in the

experiment is partially explained with the possible delay of TC response on one hand. On the other hand, axial temperature profile in the experiment may have been flatter than in the calculation. As the slug passes through TFC, the coolant channel subsequently becomes filled with the released gas (in about 20 ms). However, heat transfer between the ejected gas and channel structure cannot be modeled under the present usage of the SAS4A code. This results in a sudden step increase of the coolant temperature to the peak in the analysis work. The insufficient modeling for the possible heating of the coolant–channel structure by the gas released would not affect the results, however, because heating of the cladding after channel voiding will be dominated by the heat flow from internal fuel pellets and/or molten fuel in the coolant channel.

4.2 Cladding Failure and Gas Blowout Analysis

Comparison between analysis results by SAS4A and test data was made in Figure2, for coolant flow rates in the outlet as well as in the inlet of the test channel, at around the time of the cladding failure and subsequent gas release. It can be seen that the overall trend of flow divergence, that is the magnitude and duration of the flow rates, is well simulated by the code. In the mean time, cladding temperature reaches to about 1,000℃ at the location of failure at 460 ms after TOP . Fuel temperature remains far below the melting point at the time of the cladding failure and subsequent gas blowout. Right upon the cladding failure and initial gas blowout at 460ms after the onset of TOP, calculated flow rates increase to the peak values in step. And subsequently they gradually decline. The pin fails at around 529 ms in the analysis and the flow rates show local peaks and then continue to decrease. As the lower void front reaches the lower boundary of the channel set by the code at about 590 ms, flow stops at the inlet of the channel. The upper void front subsequently hitting the upper boundary at 680 ms or so, flow stops after a brief peak at the outlet of the channel. Void fronts, which are the integration of the flow rates, are compared in Figure 3. It can be seen that the initial rate of void development is well simulated but void fronts are delayed a bit (about 40 ms or so) in the analysis compared to what happened in the test. This may well be caused by the lack of modeling for the onset of local boiling, which appeared to have occurred in the test at 420 ms after TOP. A sudden cease of the void-front expansion is due to the limit set by the code itself for the sake of computational stability.

4.3. Pin Failure and Melt Progression Behavior

Figures 6 illustrates the melting boundary calculated at 529 ms after the triggering of TOP. The cladding temperature reached about 1,100℃ at around the failure location by this time. Fuel melting was initiated at 45 cm above BFC (core node 14) at around 500 ms after TOP. By the time of the pin failure, significant fuel melting had occurred and the axial melt front expanded from 28 cm to 56 cm above BFC. The areal melt fraction is peaked at 14 % around 45 cm BFC. Fractional radii of the melting boundary ranged from 80 to 90 %. It can be noted that fuel remains solid in the inner region while molten in outer region of the fuel pin. This represents a radial temperature inversion characteristic with the CABRI test.

Upon the pin failure at 529 ms after TOP, molten fuel is ejected from the failure node of the pin to the voided channel. The liquid sodium stays just below BFC and far above

TFC at the time of fuel ejection into the channel so that no significant fuel-coolant interaction is anticipated in this kind of TUCOP event. Right after the peak power (at 549 ms/TOP), the first fuel disruption occurs at the location of the pin failure and propagates rapidly downward along the pin. This may be well illustrated in Figure 3, which shows axial propagation of fuel disruption together with the development of the void-fronts in the channel. As can be seen, fuel disrupts extensively by 650 ms, which corresponds to the time of the end of the main power pulse with energy release reaching more than 1.0 kJ/g (80 % of the total energy). By this time, fuel disruption has propagated down to 25 cm and up to 65 cm above BFC. Fuel disruption is taking place gradually to the limited extent afterward. It is probable that the earlier TC rupture events below the failure location are more related to the ejection of molten fuel. It may be noted in the figure that the fuel disruption fronts calculated by the code reasonably well reflect a series of the events of TC rupture.

As fuel disruption progresses downward, molten fuel in the central locations down below moves upward in the pin and is ejected through the upper node into the channel and stay upward in the channel, before the central nodes disrupt for themselves at around 590 ms/TOP. As fuel disruption continues, the epicenter of the ejected fuel also moves downward. In the mean time, the plenum gas continues to be released from lower and upper ends of the pin even after the initial blowout upon cladding failure. This tends to drive the fuel and steel ejected to the either end of the fissile region.

In the end, the fuel pin disrupts to about 10 cm-long stubs from either end of the pin stay intact. The mixture of the fuel and steel is gradually relocated to the ends of the pin due to the continual release of plenum gas and gravity effect as well. Since the energy release is saturated after the scram, the relocation of the mixture of the fuel and steel tend to be limited within fissile. However, the molten steel gets relocated upward to the above of TFC. This result is consistent with a result of the PTE performing the axial cutting of the zone around TFC. However, a small amount of fuel accumulated above the molten steel as well as a few fuel fragments above TFC observed in the PTE are not predicted by the code.

Figure 7 presents a comparison of the final fuel configuration calculated by the SAS4A code to that deduced from the preliminary hodoscope data. It should be reminded that the hodoscope signal is not proportional to fuel mass due mainly to the self shielding effect. Therefore one should only compare the trend of axial fuel distribution. It can be seen in the figure that the code predicts rather well global behavior of the test data; the fuel accumulation around TFC and in the upper zone of the channel above 55 cm BFC, sharp drop of fuel at around 50 cm BFC, gradual accumulation of fuels in the central part of the core down to 30 cm BFC, and accumulation of fuel below at about 15 cm BFC. It may be noted, however, that there exist a few local deviations between the test data and the calculated results. It should be noted that the test data only shows the fuel mass increased from the steady state value. At above TFC, for instance, a small amount of increase in fuel mass would give rise to a large signal. A peak at around TFC appears to be arising from the fuel elongation occurred during TOP as well as LOF or insignificant amount of molten fuel relocation. Another peak is shown at about 30 cm BFC in the hodoscope data, while the code predicts gradual increase of fuel mass downward. Judging from the experience with the code, this appears to represent the tendency of the code to underpredict the downward fuel relocation.

5. Conclusions

An effort has been made to simulate the experimental results of the LTX test using the SAS4A code. In the test, the pin cladding failed rather early before the initiation of any significant fuel melting, presumably due to fuel pin bending. Given the time and axial location of the cladding failure and fuel ejection, the code produced the results quite consistent with the experimental results, which include the fuel disruption and melt progression behavior as well as the coolant channel voiding and subsequent heat-up of the pin. This study vindicates conclusions drawn up in the LT1 analysis [3] in terms of the ability of the code to predict the early-induced events and validity of the present treatment for dependency of the mobility of disrupted fuels on fuel enthalpy, even if the initial pin boundary conditions are quite different between the two tests.

There currently exists quite a limited amount of experimental data for the LTX test. Precision was also lost for the timing of the rupture events and their locations. For the analysis of the test, therefore, it was necessary to assume the major events by interpreting indirect information from the test. One of the major assumptions made in this study is related to the specification (time, location and mechanism) of the molten fuel ejection. That is that molten fuel starts to get ejected upon the axial separation of the cladding at around 60 cm BFC (location of the cladding failure) at 526 ms after the onset of TOP. The application of this interpretation gave rise to a simulation quite close to the experimental results of post-failure fuel behavior. The successful simulation by the SAS4A code of global behavior of the post-failure molten fuel behavior in the LTX test confirms that the code may well provide a sound basis for future evaluation of the early failure scenario in the reactor case, regardless of the details of the cladding failure.

Acknowledgement

This study has been made as part of the MEXT Scientist Exchange Program of Japan and National Long-Term Nuclear Energy Research Program of Korea in the year of 2001. The authors express their great appreciation for Mr. Katsuhiko TAKAHASHI of Nuclear Engineering System Inc.,and Mr. Takuhiro CHUBACHI of CSK INC. , who helped the analytical works and preparation of the figures.

References

[1] Y.Onoda and I.Sato, “Interpretation of the CABRI LT4 test with SAS4A-code analysis,” JNC TN9400 2001-047, March 2001

[2] Y. Fukano and I. Sato, “Interpretation of the CABRI-RAFT LTX test up to pin failure based on detailed evaluation and PAPAS-2S code analysis,” JNC TN9400 2001-xxx, September 2001

[3] I. Sato and Y. Onoda, ”Interpretation of the CABRI LT1 test with SAS4A-code analysis, “ JNC TN9400 2001-048, March 2001

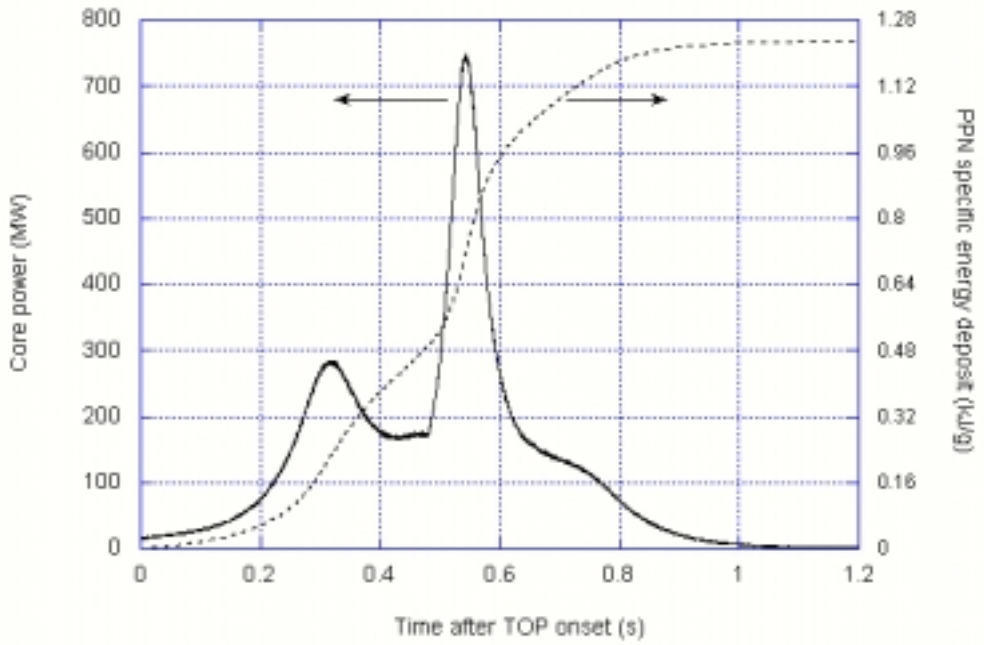

Figure 1. Power and energy release history during TOP

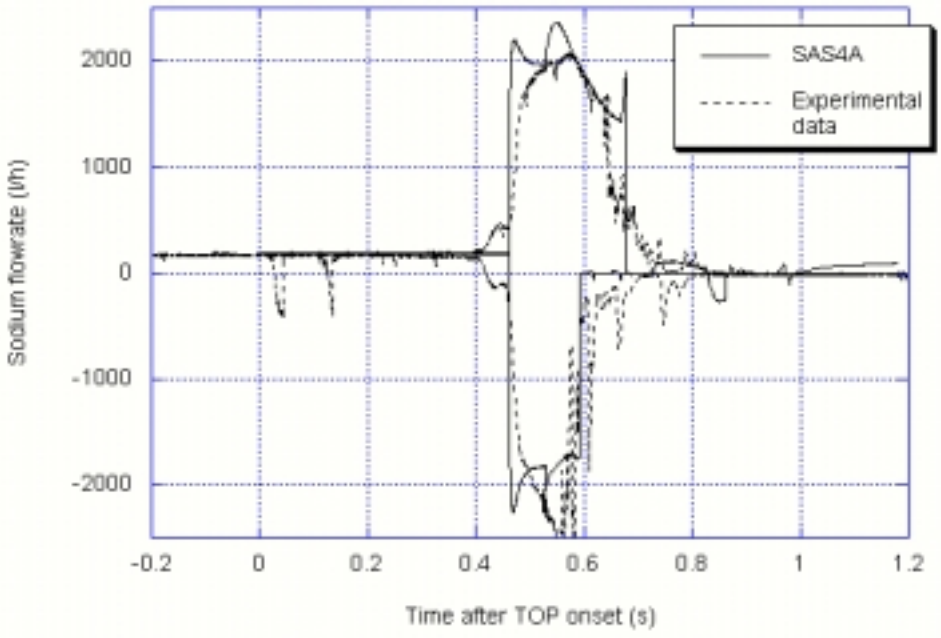

Figure 2. Coolant flow rates after the cladding failure

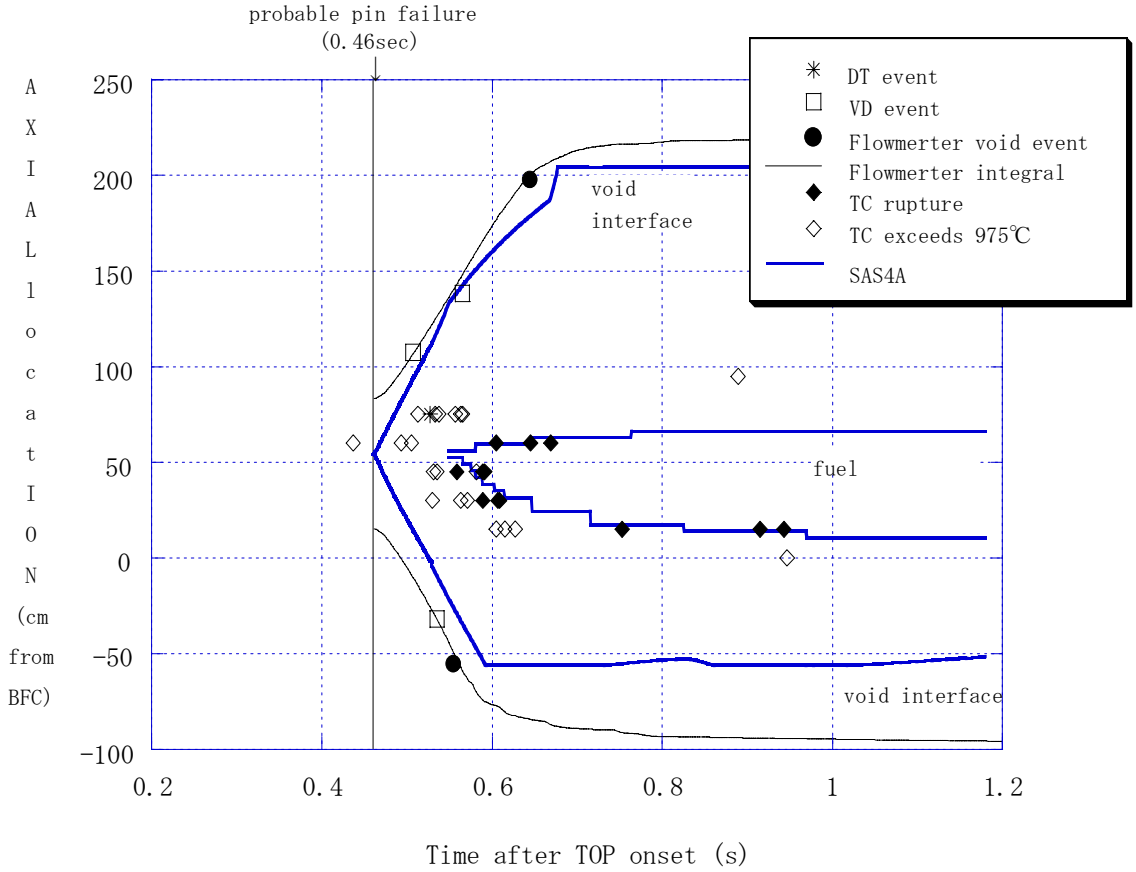

Figure 3. Coolant-channel voiding and fuel disruption fronts

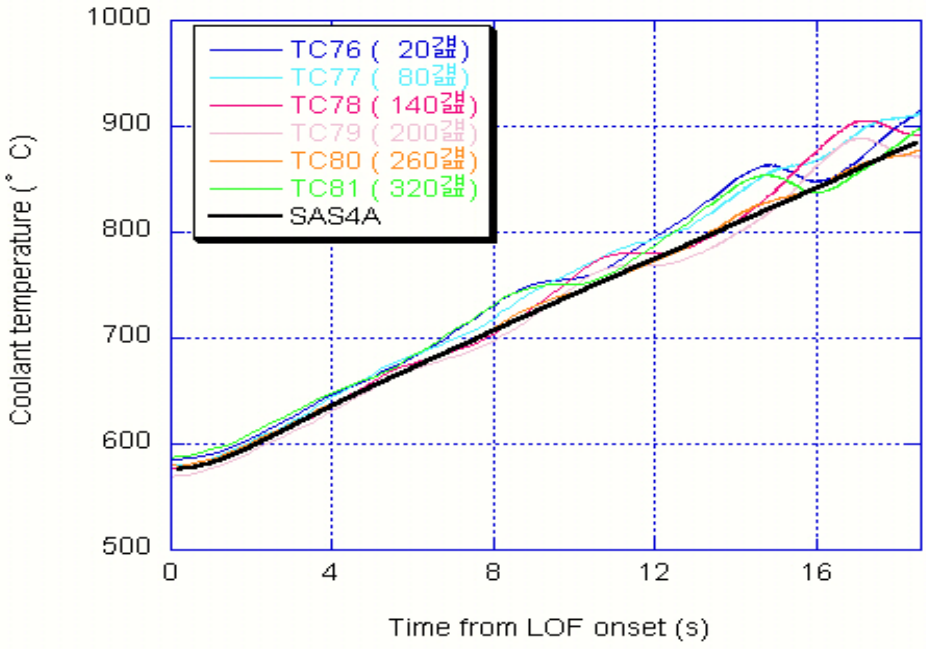

Figure 4. Comparison of coolant temperature history at TFC during LOF

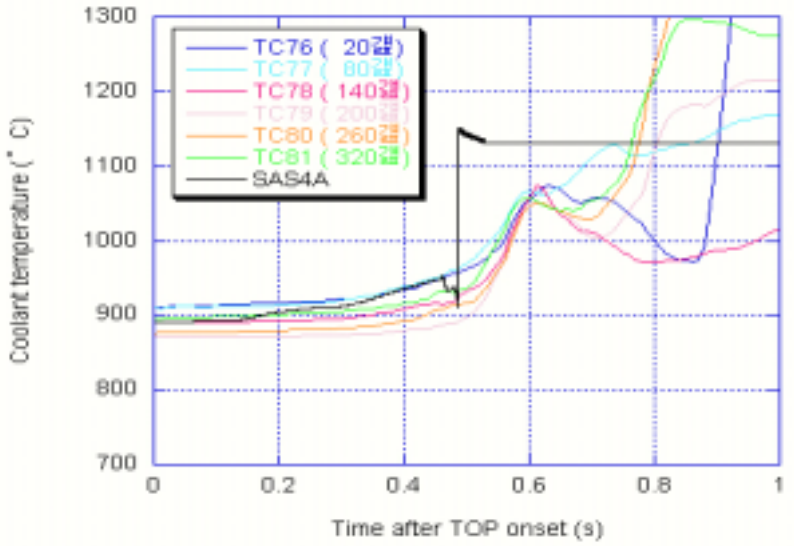

Figure 5. Coolant temperature history at TFC during TOP

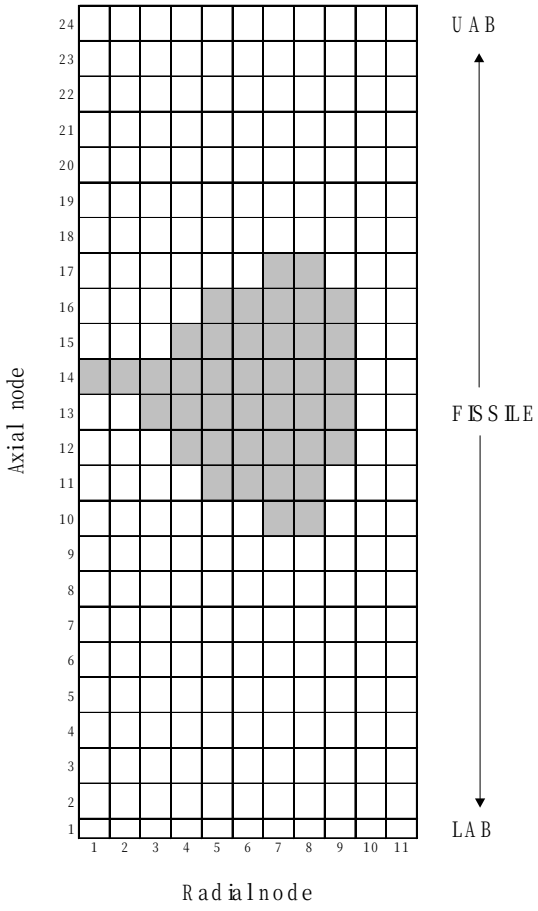

Fugure 6. Melting boundary at 530 ms after TOP

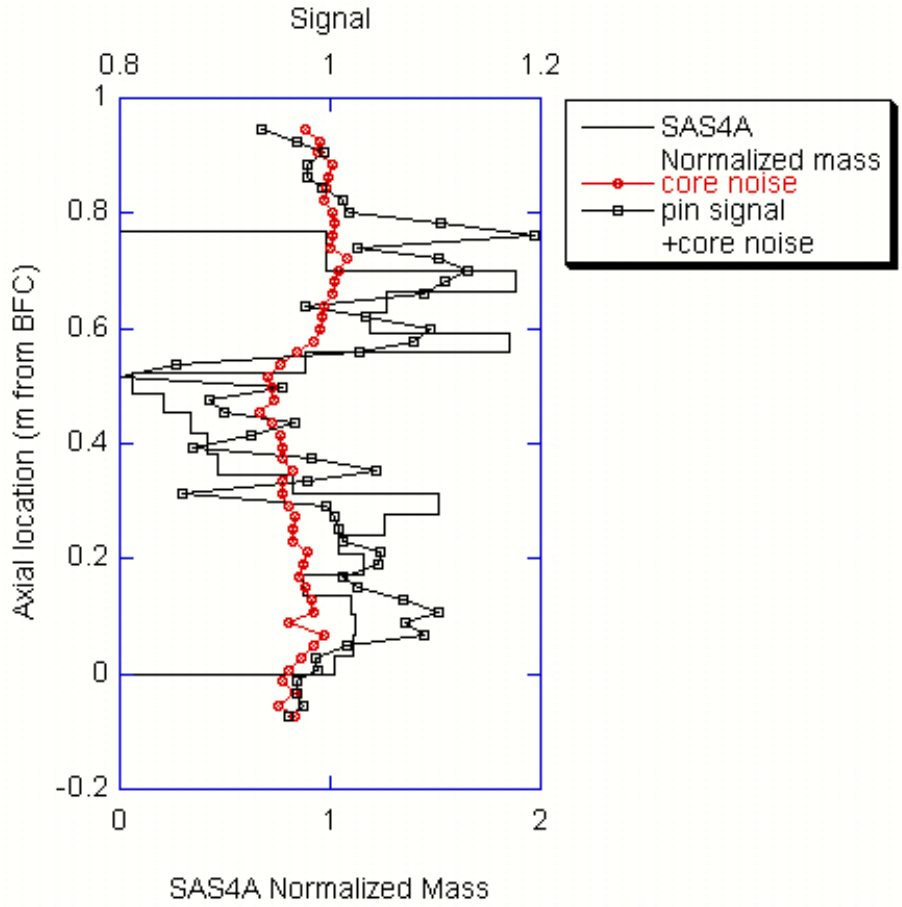

Figure 7. Comparison of final fuel configuration calculated by SAS4A to hodoscope data